


**Mode locking phenomena of the current-induced skyrmion-lattice motion in microfabricated MnSi**Takuro Sato<sup>1,\*</sup>, Akiko Kikkawa,<sup>1</sup> Yasujiro Taguchi,<sup>1</sup> Yoshinori Tokura,<sup>1,2,3</sup> and Fumitaka Kagawa<sup>1,2,†</sup><sup>1</sup>*RIKEN Center for Emergent Matter Science (CEMS), Wako 351-0198, Japan*<sup>2</sup>*Department of Applied Physics, University of Tokyo, Tokyo 113-8656, Japan*<sup>3</sup>*Tokyo College, University of Tokyo, Tokyo 113-8656, Japan* (Received 3 March 2020; revised 13 October 2020; accepted 10 November 2020; published 25 November 2020)

Using voltage fluctuation spectroscopy, we observe the mode locking phenomena of current-induced skyrmion-lattice motion in microfabricated MnSi. When only a dc electric current is applied, the frequency of the emergent narrow-band noise (NBN) monotonously increases with increasing dc current. By contrast, if an ac electric current is further added, the NBN frequency becomes much less dependent on the dc current when it satisfies a simple integer ratio to the ac current frequency, a hallmark of mode locking. In the mode locked state, the linewidth of the NBN is sharpened, indicating the enhanced coherence of the skyrmion-lattice motion. The overall features of the mode locking phenomena are qualitatively reproduced within the framework of the classical rigid-sphere model.

DOI: [10.1103/PhysRevB.102.180411](https://doi.org/10.1103/PhysRevB.102.180411)

Under a dc stimulus above a threshold value, some systems start to exhibit ac responses in such a way that the modulation frequency continuously increases with the dc driving force. One classical example is a rigid sphere moving over a tilted washboard potential: The velocity of the sphere is time variant, and its modulation frequency is dictated by the ratio between the mean velocity and the spatial periodicity of the potential. Similar phenomena can also be seen in solids. When an external force drives a certain long-range order, such as charge/spin density waves and flux-line lattices in type-II superconductors, the velocity is modulated at certain frequencies. This modulation is observed as the so-called narrow-band noise (NBN) in the frequency domain, and in this case, the spatial periodicity of the order plays a key role in the emergent oscillation [1–6]. The external-force-induced dynamics may acquire a rich variety when an ac driving force is superimposed. Specifically, it is known that plateau responses may appear in the otherwise smoothly varying dc force–frequency curve, in such a way that the frequencies of NBN,  $f_{\text{NBN}}$ , and the external ac force,  $f_{\text{ex}}$ , satisfy  $f_{\text{NBN}}/f_{\text{ex}} = p/q$ , where  $p$  and  $q$  are both small integers. This phenomenon may be viewed as a complex interference between the dc-driven spontaneous and ac-driven forced oscillations, often referred to as mode locking [7–10].

Very recently, a new class of a long-range order, a magnetic skyrmion lattice, has been found to exhibit NBN in the power spectral density of voltage fluctuations (abbreviated as voltage PSD below) when the external dc electric current density exceeds a certain threshold value [11]. Magnetic skyrmions are topologically protected, spin-swirling objects with diameters in the range of 5–100 nm and can condense in a close-packing manner [12–15]. The resulting

skyrmion triangular lattice can thus be viewed as a long-range order with a spatial periodicity of, approximately, the skyrmion diameter. Moreover, skyrmions are found to be driven by an electric current through the spin-transfer torque [16–25], and a skyrmion lattice therefore provides a good platform to address the external-force-induced nonlinear dynamics mentioned above. In fact, numerical simulations on a skyrmion lattice have predicted both NBN under a dc driving force [26–28] and its mode locking phenomena under dc + ac driving forces [29,30]. Nevertheless, the mode locking phenomena of skyrmion-lattice motion remain to be experimentally verified, and furthermore, it is not clear how the addition of an ac electric current affects the coherence of the skyrmion-lattice motion under the influence of a random pinning potential.

In this Rapid Communication, to reveal how the superposition of an ac current modifies the dc-current-induced NBN in the skyrmion lattice, we perform voltage fluctuation spectroscopy. For a given  $f_{\text{ex}}$  and ac electric current,  $j_{\text{ac}}$ , we find that several plateaus emerge in the dc current–NBN frequency ( $j_{\text{dc}}-f_{\text{NBN}}$ ) profile when  $f_{\text{NBN}}/f_{\text{ex}} = p/q$  is satisfied. These observations are qualitatively in line with what is observed for mode locking phenomena in different systems, and we thus conclude the experimental realization of the mode locking phenomena in current-induced skyrmion-lattice motion. The plateau width depends on  $j_{\text{ac}}$ , and its variations are found to be reproduced well within the framework of the phenomenological rigid-sphere model, indicating that the classical model provides a good basis for the qualitative understanding of skyrmion-lattice dynamics.

The schematic of the experimental setup is shown in Fig. 1(a). The measurements were performed on a microfabricated MnSi specimen, and the sample size was  $14 \times 1 \times 0.8 \mu\text{m}^3$ . The magnetic state of the specimen was put in the skyrmion-lattice phase by applying a certain magnetic field parallel to the substrate and perpendicular to the current

\*takuro.sato@riken.jp

†kagawa@ap.t.u-tokyo.ac.jp

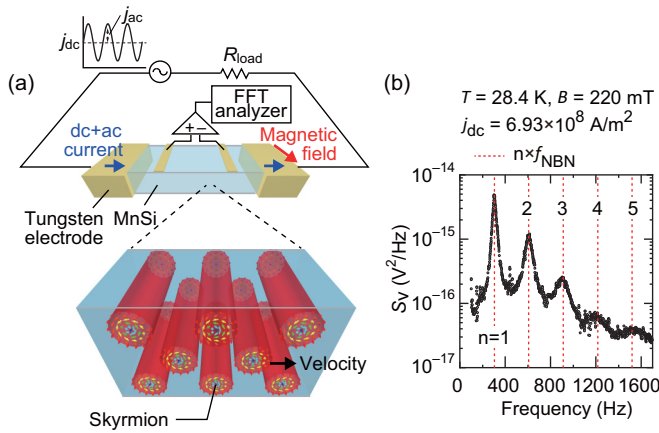


FIG. 1. (a) Schematic of the experimental configurations. An external magnetic field is applied parallel to the substrate and perpendicular to the long axis of the bar-shaped sample. The electric current is applied along the long axis. The corresponding scanning electron microscope image is shown in Fig. S1 in the Supplemental Material [31]. (b) Typical power spectral density of voltage fluctuations for the narrow-band noise in the skyrmion-lattice phase under the application of a dc electric current above a threshold value. The spectrum exhibits several higher harmonic bands, of which the frequencies agree with the integral multiple of the fundamental NBN frequency,  $f_{\text{NBN}}$ .

direction (for the magnetic phase diagram of the specimen, see Fig. S1 in the Supplemental Material [31]). We measured a series of voltage PSDs,  $S_V(f)$ , under dc + ac electric currents using a spectrum analyzer (for details, see the Methods section in the Supplemental Material [31]). The specimen exhibits NBN emerging from the dc-current-induced skyrmion-lattice motion when  $j_{\text{dc}}$  exceeds  $\sim 5 \times 10^8 \text{ A/m}^2$  [11]. When the ac electric current was absent, higher harmonic NBN was discerned up to the fifth band, and a complex coexistence of other bands was not observed [Fig. 1(b)]. All the data below were obtained at  $T = 28.4 \text{ K}$  and  $B = 220 \text{ mT}$  (in the skyrmion phase), and we investigated the  $j_{\text{dc}}-f_{\text{NBN}}$  profile under the influence of an ac electric current of  $f_{\text{ex}} = 700 \text{ Hz}$ .

Figures 2(a) and 2(b) display  $S_V(f)$  profiles in the absence and presence of  $j_{\text{ac}}$  ( $= 2 \times 10^8 \text{ A/m}^2$ ), respectively, for the conditions that  $f_{\text{NBN}}$  appears near  $350 \text{ Hz}$  ( $= f_{\text{ex}}/2$ ). When  $j_{\text{ac}} = 0$  [Fig. 2(a)], the peak frequency of the fundamental NBN continuously shifts toward higher frequencies as  $j_{\text{dc}}$  increases, whereas its spectral shape stays approximately symmetric, as observed in our previous study [11].

The behavior dramatically changes when the finite  $j_{\text{ac}}$  is superimposed, and as detailed below, the voltage PSD shows complex variations against continuous change in  $j_{\text{dc}}$ . When  $f_{\text{NBN}}$  is appreciably lower than  $f_{\text{ex}}/2$  [PSD (I) in Fig. 2(b)], the PSD is symmetric and rather broadened compared with the case of  $j_{\text{ac}} = 0$ . It demonstrates that the coherence of the dc-current-induced skyrmion-lattice motion is somewhat disturbed by the addition of off-resonant  $j_{\text{ac}}$ . As  $f_{\text{NBN}}$  approaches  $f_{\text{ex}}/2$  [PSD (II)], the spectral shape becomes distorted and the spectral weight is pulled toward  $f_{\text{ex}}/2$ . Such behavior, referred to as the “frequency-pulling effect,” has been reported as a precursor phenomenon of mode locking in charge-density-wave (CDW) systems [32,33]. When  $f_{\text{NBN}}$  matches  $f_{\text{ex}}/2$ ,

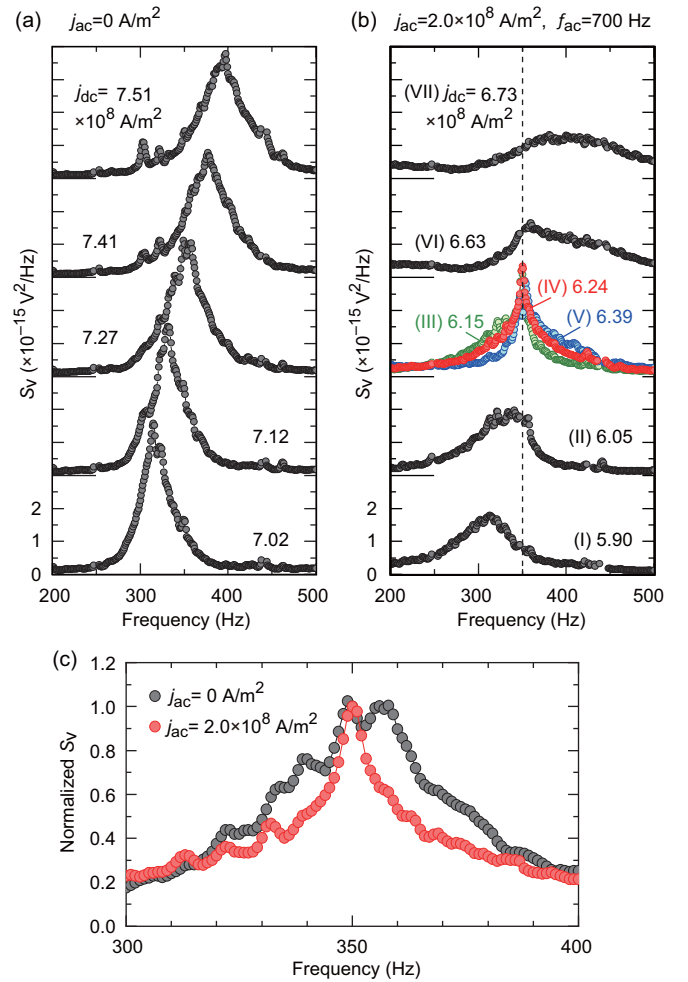


FIG. 2. (a), (b) Power spectral densities (PSDs) of voltage fluctuations in the (a) absence and (b) presence of an ac electric current. (c) Comparison between the NBN spectra in the absence of an ac electric current ( $j_{\text{dc}}$  and  $j_{\text{ac}}$  are  $7.27 \times 10^8$  and  $0 \text{ A/m}^2$ , respectively) and in the mode locked state in the presence of an ac electric current ( $j_{\text{dc}}$  and  $j_{\text{ac}}$  are  $6.24 \times 10^8$  and  $2.0 \times 10^8 \text{ A/m}^2$ , respectively).

the PSD exhibits a pronouncedly sharp peak. Remarkably, the peak frequency remains unchanged for a finite range of increase in  $j_{\text{dc}}$ , although the spectral weight continues to shift toward higher frequencies [PSD (III to V)]; that is, the peak frequency is “locked” into  $f_{\text{ex}}/2$ . The linewidth is appreciably narrower than that of  $j_{\text{ac}} = 0$  [Fig. 2(c)], indicating that the coherence of the current-induced motion of the skyrmion lattice is rather enhanced in the locking condition. As  $j_{\text{dc}}$  is increased further,  $f_{\text{NBN}}$  becomes “unlocked” and starts to shift toward higher frequencies [PSD (VI)], and eventually, the spectrum reverts to a broadened symmetric shape [PSD (VII)]. The systematic variations in the linewidths as a function of  $j_{\text{dc}}$  are summarized in Fig. S3 in the Supplemental Material [31].

The locking-unlocking transition can be seen more clearly when the  $j_{\text{dc}}-f_{\text{NBN}}$  profile is derived from Figs. 2(a) and 2(b). The results are shown in Fig. 3, comparing the  $j_{\text{dc}}-f_{\text{NBN}}$  profiles in the presence and absence of  $j_{\text{ac}}$ . When  $j_{\text{ac}} = 0$ ,  $f_{\text{NBN}}$  smoothly increases as a function of  $j_{\text{dc}}$ , as previously reported [11]. When the ac electric current is present, however,

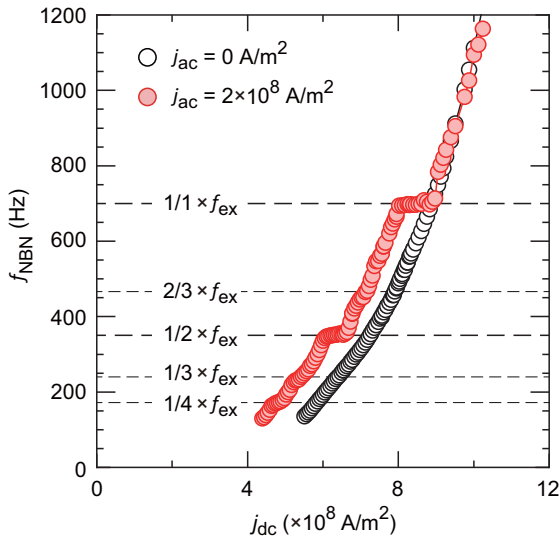


FIG. 3. dc current density dependence of  $f_{\text{NBN}}$  with and without externally applied ac current at  $f_{\text{ex}} = 700$  Hz (red and black plot, respectively), measured at the skyrmion phase. The staircase structures are labeled with a set of small integers.

multiple step structures appear in such a way that  $f_{\text{NBN}}$  satisfies the relation  $f_{\text{NBN}}/f_{\text{ex}} = p/q$ . Such anomalies are referred to as a harmonic step for  $p/q = \text{integer}$  and a subharmonic step for  $p/q = \text{noninteger}$ . In each step, the  $j_{\text{dc}}-f_{\text{NBN}}$  profile exhibits either a plateau ( $p/q = 1/1$  and  $1/2$ ) or kink ( $p/q = 2/3, 1/3$ , and  $1/4$ ), thus indicating an interplay between the time-varying skyrmion-lattice motion induced by dc current and a forced oscillating motion induced by ac current. Similar staircase behavior is observed in other systems as a signature of mode locking [1,32], and we therefore conclude that the mode locking in the current-induced motion of the skyrmion lattice is experimentally demonstrated.

In the mode locking observed in CDW systems, the plateau behavior in the  $j_{\text{dc}}-f_{\text{NBN}}$  profile is often smeared and turns into kinklike anomalies when the sample quality is moderate, and thus the spatial and temporal phase coherence of the CDW motion is considered to be crucial for mode locking [1]. On the basis of this knowledge, the observation of the clear plateau in the present study indicates that the skyrmion-lattice motion in the microfabricated MnSi has relatively high coherence. Nevertheless, the quantitative estimation of the dynamic coherence length is experimentally challenging, and the nature and origin of the pinning are currently not clear; more specifically, it remains unclear whether the system is in a strong or weak pinning regime [1] and whether the pinning arises from bulk impurities or surface barriers that affect the skyrmion flow into and out of the sample edges.

Given the lack of microscopic insight into the pinning, here, we take a phenomenological approach and analyze the results within the classical rigid-sphere model. When adopting this model, we neglected the meandering degree of freedom in the skyrmion string [34] and correlations along the direction perpendicular to the skyrmion-string flow. With this assumption, we map the skyrmion lattice of the periodicity of  $\approx 20$  nm in the presence of the pinning potential onto a rigid sphere in the presence of a periodic effective potential of the periodicity

of  $\approx 20$  nm. The equation of motion of the rigid sphere is thus given as

$$m \frac{d^2x}{dt^2} + \gamma \frac{dx}{dt} + \frac{dU(x)}{dx} = \eta j(t), \quad (1)$$

where  $m$  is the mass of the rigid sphere (or, equivalently, the phenomenological mass of the skyrmion lattice),  $\gamma$  is a damping constant,  $U(x)$  is a one-dimensional periodic potential, and  $\eta$  is a given coupling term between the driving force and the applied current; for details, see Sec. V in the Supplemental Material [31]. In the simplest case, one can take a cosine potential as  $U(x) = -k \left(\frac{\lambda}{2\pi}\right)^2 \cos\left(\frac{2\pi}{\lambda}x\right)$ , where  $\lambda$  is a periodicity and  $k$  is a restoring-force constant. When we chose the parameters  $k$  and  $\gamma$  such that the experimentally observed threshold current density and slope of the  $j_{\text{dc}}-f_{\text{NBN}}$  profile are reproduced, we find that this simplest model shows nonlinear dynamics, such as velocity modulation (i.e., NBN) under a dc force and its mode locking phenomena under the addition of an ac force (Fig. S8 in the Supplemental Material [31]). Thus, the model seems successful in describing the skyrmion-lattice dynamics under time-varying electric currents. We also note that the equation of motion [Eq. (1)] is formally identical to the equation that describes the behavior of resistively shunted Josephson junctions [1], in which corresponding phenomena, such as Shapiro steps, are also observed [35]. Note that the microscopic derivation of Eq. (1) is still lacking for the cases of the dynamics of the flux-line lattice, CDW, and skyrmion lattice [7,36].

To further test this phenomenological model, it is important to explore a phenomenon that has not been confirmed by experiments but is predicted from Eq. (1). One such intriguing prediction is that the width of the emergent “1/1” harmonic step in the  $j_{\text{dc}}-f_{\text{NBN}}$  profile,  $\Delta j_{\text{dc}}$ , varies in an oscillating manner as a function of  $j_{\text{ac}}$  [4,7,37],

$$\Delta j_{\text{dc}} \approx 2\alpha j_c \left| J_1 \left( \frac{\beta j_{\text{ac}}}{j_c} \right) \right|, \quad (2)$$

where  $J_1$  is the first-ordered Bessel function,  $j_c$  is a threshold current density in the absence of  $j_{\text{ac}}$ ,  $\beta$  is a dimensionless fitting parameter, and  $\alpha$  ( $0 \leq \alpha \leq 1$ ) is a phenomenological scale factor that describes the difference in the results between the rigid-sphere model and real experiments ( $\alpha = 1$  corresponds to the plateau width of the rigid-sphere model, and thus  $\alpha$  is often regarded as a parameter that describes a volume fraction responding to the external driving forces [4,7,37]). Thus, examining whether the experimental  $j_{\text{ac}}-\Delta j_{\text{dc}}$  profile can reproduce such an oscillating step width emergent from the model [Eq. (2)] is a more stringent test for the validity of the rigid-sphere model in the context of the mode locking of the skyrmion-lattice motions.

We analyzed the variations in the  $\Delta j_{\text{dc}}$  of the 1/1 harmonic step as a function of  $j_{\text{ac}}$ , as shown in Figs. 4(a) and 4(b). We estimated the plateau width in two ways: (i) directly from the locking of the fundamental peak at 700 Hz [Fig. 4(a)] and (ii) indirectly from the locking of the sum-frequency sideband at 1400 Hz ( $= f_{\text{NBN}} + f_{\text{ex}}$ ) (see Fig. S7 in the Supplemental Material [31]). While the number of available data points is limited for case (i), the analysis based on (ii) enables us to analyze the plateau width up to higher  $j_{\text{ac}}$  (for details,

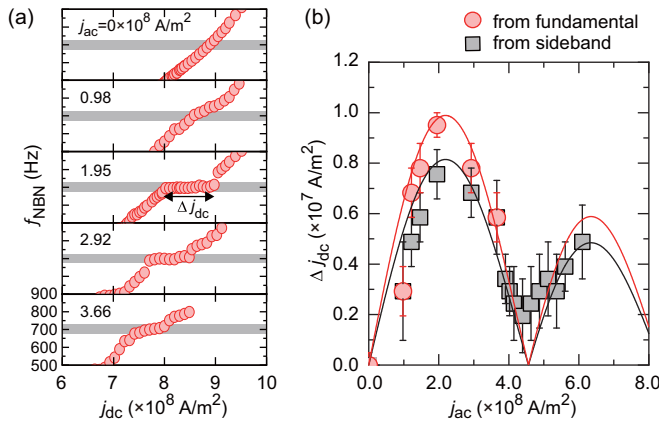


FIG. 4. (a) dc current density dependence of  $f_{\text{NBN}}$  approximately 700 Hz at representative magnitudes of an ac current of 700 Hz. We defined the widths of the 1/1 harmonic step of the mode locking  $\Delta j_{\text{dc}}$  as the range of  $j_{\text{dc}}$  in which the fundamental NBN is within  $700 \pm 25$  Hz (highlighted by gray shaded regions). (b)  $j_{\text{ac}}$  dependence of  $\Delta j_{\text{dc}}$ . Red and black points are derived from (a) and the analysis of sum-frequency sideband (see Fig. S7 in the Supplemental Material [31]), respectively. Red and black lines are fits of Eq. (2).

see Fig. S5 in the Supplemental Material [31]). Overall, the results are consistent with each other, and both  $\Delta j_{\text{dc}}$  show an oscillating behavior against  $j_{\text{ac}}$  [Fig. 4(b)]. More importantly, this behavior is fitted well by Eq. (2) (the red and black curves), demonstrating that the classical rigid-sphere model describes the mode locking of skyrmion-lattice motion well. The derived  $\alpha$  values are 0.17 and 0.14 for analysis procedures (i) and (ii), respectively. These values are comparable to those of high-purity CDW systems ( $\alpha \approx 0.17$ ) [7], again suggesting that the skyrmion-lattice motion in microfabricated MnSi has a relatively high spatiotemporal coherence.

Finally, we focus on the emergence of the subharmonic steps and discuss its physical implications within the framework of the classical rigid-sphere model (for a more elaborated approach, see Refs. [38,39]). Numerical simulations of the rigid-sphere model tell us that (i) as long as a single-component cosine potential is considered, finite mass is absolutely essential for the emergence of subharmonic steps (Fig. S8 in the Supplemental Material [31]; see also Refs. [40,41]), and (ii) alternatively, even if the mass is zero or negligibly small, the subharmonic steps can appear when the effective potential includes higher-order cosine components (Fig. S8 in the Supplemental Material [31]). Thus, the emergence of the subharmonic steps in the skyrmion-lattice mode locking is likely accounted for by considering a higher-order cosine effective potential for the skyrmion-lattice motion and/or a finite phenomenological mass in Eq. (1).

In this context, we note that the steady flow of skyrmions in such a microscaled specimen is presumably significantly influenced by the creation and/or annihilation rates of skyrmions at the sample edges [11]. When reducing to the rigid-sphere model, such singular events at the edges would give rise to higher-order cosine components as well as a fundamental one in the effective potential, thus reasonably

accounting for the emergence of the subharmonic step. Even if we neglect such singularities arising from the edges, neutron diffraction experiments revealed weak but appreciable higher harmonic Bragg spots in a skyrmion lattice [16], indicating that the effective potential in a rigid-sphere model should include higher-order cosine components.

Nevertheless, we do not rule out the possibility that the phenomenological mass in Eq. (1) is finite. While magnetic skyrmions are often regarded as nearly massless [12,25], some theoretical studies note that a two-dimensional (2D) single skyrmion may have an extremely small but finite effective mass  $m_{\text{single}}^{2\text{D}}$  ( $\sim 10^{-25}$  to  $\sim 10^{-24}$  kg) due to its internal deformation [42] or a confining potential [43]. If we tentatively fit the experimental results to the rigid-sphere model with a single cosine potential, we find that the phenomenological mass  $m$  in Eq. (1) is  $\sim 10^{-11}$  kg, 14 orders of magnitude larger than the theoretically predicted  $m_{\text{single}}^{2\text{D}}$  (Fig. S8 in the Supplemental Material [31]). On one hand, this large discrepancy seemingly suggests that the value of the phenomenological mass is not reasonable and thus the experimental observation of the subharmonic step should be ascribed to a higher-order cosine effective potential. On the other hand, given that we derived the phenomenological mass for a three-dimensional (3D) skyrmion lattice [Fig. 1(a)], a comparison to the microscopically predicted  $m_{\text{single}}^{2\text{D}}$  for an isolated 2D skyrmion is not straightforward. Furthermore, even if we limit the discussion only to a microscopic level, the relationship between  $m_{\text{single}}^{2\text{D}}$  and the mass of a 3D skyrmion lattice  $m_{\text{lattice}}^{3\text{D}}$  is not clear at this moment. During the flow motion, the internal deformations of a 3D skyrmion string and an interaction between skyrmion strings may need to be considered. These issues are beyond the scope of the present experiment, and we leave this to future independent theoretical works.

In conclusion, we performed voltage fluctuation spectroscopy on a microfabricated MnSi under dc + ac electric current and demonstrated the mode locking phenomena of current-induced skyrmion-lattice motion. In the mode locked state, the linewidth of NBN is sharpened, indicating the enhanced coherence of the motion. The mode locking phenomena of the magnetic skyrmion lattice are qualitatively reproduced within the framework of the classical rigid-sphere model, and the physical implications of the emergence of the subharmonic step are discussed. The classical model validated here has been widely applied to a broad class of systems, such as CDW, flux-line lattices in type-II superconductors, and resistively shunted Josephson junctions. We thus expect that a perspective based on this model would provide a facile method to describe the skyrmion-lattice dynamics under time-varying electric currents. Nevertheless, as the microscopic derivation of the classical rigid-sphere model is lacking, there still remains a possibility that a phenomenological model in a different form is more suitable for describing the 3D skyrmion-lattice dynamics.

T.S. and F.K. thank S. Okuma, W. Koshibae, S. Kaneko, and K. Ienaga for their valuable discussions. This work was partially supported by JSPS KAKENHI (Grants No. 20H01866, No. 18H05225, and No. 18K13510) and JST CREST Grants No. JPMJCR1874 and No. JPMJCR20T1, Japan.

- [1] G. Grüner, *Rev. Mod. Phys.* **60**, 1129 (1988).
- [2] P. Monceau, *Adv. Phys.* **61**, 325 (2012).
- [3] R. M. Fleming and C. C. Grimes, *Phys. Rev. Lett.* **42**, 1423 (1979).
- [4] M. F. Hundley and A. Zettl, *Phys. Rev. B* **39**, 3026 (1989).
- [5] T. Sekine, N. Satoh, M. Nakazawa, and T. Nakamura, *Phys. Rev. B* **70**, 214201 (2004).
- [6] Y. Togawa, R. Abiru, K. Iwaya, H. Kitano, and A. Maeda, *Phys. Rev. Lett.* **85**, 3716 (2000).
- [7] A. Zettl and G. Grüner, *Phys. Rev. B* **29**, 755 (1984).
- [8] R. P. Hall and A. Zettl, *Phys. Rev. B* **30**, 2279(R) (1984).
- [9] S. E. Brown, G. Mozurkewich, and G. Grüner, *Phys. Rev. Lett.* **52**, 2277 (1984).
- [10] M. S. Sherwin and A. Zettl, *Phys. Rev. B* **32**, 5536(R) (1985).
- [11] T. Sato, W. Koshibae, A. Kikkawa, T. Yokouchi, H. Oike, Y. Taguchi, N. Nagaosa, Y. Tokura, and F. Kagawa, *Phys. Rev. B* **100**, 094410 (2019).
- [12] N. Nagaosa and Y. Tokura, *Nat. Nanotechnol.* **8**, 899 (2013).
- [13] S. Mühlbauer, B. Binz, F. Jonietz, C. Pfleiderer, A. Rosch, A. Neubauer, R. Georgii, and P. Böni, *Science* **323**, 915 (2009).
- [14] W. Münzer, A. Neubauer, T. Adams, S. Mühlbauer, C. Franz, F. Jonietz, R. Georgii, P. Böni, B. Pedersen, M. Schmidt, A. Rosch, and C. Pfleiderer, *Phys. Rev. B* **81**, 041203(R) (2010).
- [15] X. Z. Yu, Y. Onose, N. Kanazawa, J. H. Park, J. H. Han, Y. Matsui, N. Nagaosa, and Y. Tokura, *Nature (London)* **465**, 901 (2010).
- [16] F. Jonietz, S. Mühlbauer, C. Pfleiderer, A. Neubauer, W. Münzer, A. Bauer, T. Adams, R. Georgii, P. Böni, R. A. Duine, K. Everschor, M. Garst, and A. Rosch, *Science* **330**, 1648 (2010).
- [17] T. Schulz, R. Ritz, A. Bauer, M. Halder, M. Wagner, C. Franz, C. Pfleiderer, K. Everschor, M. Garst, and A. Rosch, *Nat. Phys.* **8**, 301 (2012).
- [18] X. Z. Yu, N. Kanazawa, W. Z. Zhang, T. Nagai, T. Hara, K. Kimoto, Y. Matsui, Y. Onose, and Y. Tokura, *Nat. Commun.* **3**, 998 (2012).
- [19] A. Fert, V. Cros, and J. Sampaio, *Nat. Nanotechnol.* **8**, 152 (2013).
- [20] J. Sampaio, V. Cros, S. Rohart, A. Thiaville, and A. Fert, *Nat. Nanotechnol.* **8**, 839 (2013).
- [21] J. Iwasaki, M. Mochizuki, and N. Nagaosa, *Nat. Commun.* **4**, 1463 (2013).
- [22] J. Iwasaki, M. Mochizuki, and N. Nagaosa, *Nat. Nanotechnol.* **8**, 742 (2013).
- [23] S. Woo, K. Litzius, B. Krüger, M.-Y. Im, L. Caretta, K. Richter, M. Mann, A. Krone, R. M. Reeve, M. Weigand, P. Agrawal, I. Lemesch, M.-A. Mawass, P. Fischer, M. Kläui, and G. S. D. Beach, *Nat. Mater.* **15**, 501 (2016).
- [24] W. Jiang, X. Zhang, G. Yu, W. Zhang, X. Wang, M. B. Jungfleisch, J. E. Pearson, X. Cheng, O. Heinonen, K. L. Wang, Y. Zhou, A. Hoffmann, and S. G. E. te Velthuis, *Nat. Phys.* **13**, 162 (2017).
- [25] K. Litzius, I. Lemesch, B. Krüger, P. Bassirian, L. Caretta, K. Richter, F. Büttner, K. Sato, O. A. Tretiakov, J. Förster, R. M. Reeve, M. Weigand, L. Bykova, H. Stoll, G. Schütz, and G. S. D. Beach, *Nat. Phys.* **13**, 170 (2017).
- [26] S. A. Díaz, C. J. O. Reichhardt, D. P. Arovas, A. Saxena, and C. Reichhardt, *Phys. Rev. B* **96**, 085106 (2017).
- [27] C. Reichhardt, D. Ray and C. J. O. Reichhardt, *Phys. Rev. Lett.* **114**, 217202 (2015).
- [28] C. Reichhardt and C. J. Olson Reichhardt, *New J. Phys.* **18**, 095005 (2016).
- [29] C. Reichhardt and C. J. O. Reichhardt, *Phys. Rev. B* **92**, 224432 (2015).
- [30] C. Reichhardt and C. J. O. Reichhardt, *Phys. Rev. B* **95**, 014412 (2017).
- [31] See Supplemental Material at <http://link.aps.org/supplemental/10.1103/PhysRevB.102.180411> for the details of methods and supplemental data.
- [32] S. Bhattacharya, J. P. Stokes, M. J. Higgins, and R. A. Klemm, *Phys. Rev. Lett.* **59**, 1849 (1987).
- [33] S. Bhattacharya, M. J. Higgins, and J. P. Stokes, *Phys. Rev. B* **38**, 7177(R) (1988).
- [34] T. Yokouchi, S. Hoshino, N. Kanazawa, A. Kikkawa, D. Morikawa, K. Shibata, T. Arima, Y. Taguchi, F. Kagawa, N. Nagaosa, and Y. Tokura, *Sci. Adv.* **4**, eaat1115 (2018).
- [35] S. P. Benz, M. S. Rzchowski, M. Tinkham, and C. J. Lobb, *Phys. Rev. Lett.* **64**, 693 (1990).
- [36] G. Grüner and A. Zettl, *Phys. Rep.* **119**, 117 (1985).
- [37] A. Zettl and G. Grüner, *Solid State Commun.* **46**, 501 (1983).
- [38] S. N. Coppersmith and P. B. Littlewood, *Phys. Rev. Lett.* **57**, 1927 (1986).
- [39] P. F. Tua and J. Ruvalds, *Solid State Commun.* **54**, 471 (1985).
- [40] M. Y. Azbel and P. Bak, *Phys. Rev. B* **30**, 3722 (1984).
- [41] J. Tekić, A. E. Botha, P. Mali, and Y. M. Shukrinov, *Phys. Rev. E* **99**, 022206 (2019).
- [42] C. Schütte, J. Iwasaki, A. Rosch, and N. Nagaosa, *Phys. Rev. B* **90**, 174434 (2014).
- [43] J. Iwasaki, W. Koshibae, and N. Nagaosa, *Nano Lett.* **14**, 4432 (2014).